SEISMIC RESIDUAL STATIC CORRECTION USING BEADS

ZAHRA SADEGHI, ALIREZA GOUDARZI, PARVANEH PAKMANESH and SADEGH MOGHADDAM

Department of Geophysics, Graduate University of Advanced Technology, Kerman, Iran. Goudarzi.kgut@gmail.com.

(Received June 9, 2021; revised version accepted December 13, 2021)

ABSTRACT

Sadeghi, Z., Goudarzi, A., Pakmanesh, P. and Moghaddam, S., 2022. Seismic residual static correction using BEADS. *Journal of Seismic Exploration*, 31: 65-80.

When seismic waves propagate through layers close to the surface, topography and velocity variations, as well as the thickness of this layer, change the shape of the travel-time hyperbolas. These deviations are known as static and cause misalignment and loss events in the CMP gathers, so estimating residual statics in complex areas is one of the greatest challenges in seismic data processing, and the results derived from them will affect the quality of the final reconstructed image and the results of the interpretation. In this research, at least in the category of seismic data processing, sparsity for the residual static correction is implemented for the first time. Baseline estimation and denoising using sparsity (BEADS) is based on modeling the series of seismogram peaks, as sparse with sparse derivatives, and additionally on modeling the datum as a low-pass signal. This method estimates the seismogram datum and residual static correction with sparsity and it's far assessed through evaluating with Gaussian smoothing that is a traditional method, using both synthetic and real seismic data.

KEY WORDS: residual static correction, sparsity, datum correction, sparse derivative, penalty function, low-pass filtering.

INTRODUCTION

There are numerous sources of ambiguities that affect the quality and the overall performance of seismic data analysis (Smite and Steigstra, 1988; Barwick, 1998). As with many different analytical methods, seismic data measurements regularly take into consideration a combination of peaks, background, and noise (McNulty and MacFie, 1998). Peak line shapes may

0963-0551/22/$5.00

also have different natures, which include Gaussian or asymmetric experimental models (Felinger, 1998). Problems with smooth datum and statics are resolved in different steps (Laeven and Smit, 1985): a generally low-order approximation or smoothing for the datum, and varieties of filtering (Brown et al., 2000). Although it appears simple, the troubles of datum subtraction and static correction stay a long-status subject.

Methods based on linear and non-linear (Moore and Jorgenson, 1993; Kneen and Annegarn, 1996; Ruckstuhl et al., 2001) filtering or multi-scale varieties of filtering with wavelet transform (Chau and Leung, 2000; Hu et al., 2007; Cappadona et al., 2008; Liu et al., 2013) had been suggested. The relative overlap between the peak spectra, the datum, and the noise has led to alternative regression models, based on different limitations. The low-pass section of the datum can be modeled with regular functions along with low-degree polynomials (Mazet et al., 2005; Zhang et al., 2010) or (cubic) spline models (Fischer et al., 2000; Gulam Razul et al., 2003; de Rooi and Eilers, 2012) in conjunction with manual identification, polynomial fitting, or iterative thresholding methods (Gan et al., 2006). Many algorithms based on sparsity had been developed for reconstructing, denoising, detection, deconvolution. Most sparse modeling strategies are derived from the least absolute shrinkage and selection operator, basis pursuit methods (Chen et al., 1998), total variation (Chan et al., 2001), and compound regularization (Bioucas-Dias and Figueiredo, 2008). The non-linear evaluation is denominated "morphological component analysis", "geometric separation" or "clustered sparsity" (Kutyniok, 2014). Most datum signals in practice now do no longer observe polynomial laws faithfully over an extended range. Therefore, we practice a model of slowly converting datum drifts as a low-pass signal. Low-pass datum models are more flexible and suitable for figuring out the behavior of the smoothing operator than polynomial approximations or symmetry lines.

Since 1960, numerous techniques have been introduced for residual static correction. Some of those techniques are based on the inversion of arrival times and acquiring the desired displacement for the effects of source and receivers (Wiggins et al., 1976; Hatherly et al., 1994). Other static residual correction strategies using minimizing an error function that is acquired from linear inversion of deviation of arrived time, those strategies had insufficient overall performance (Ronen and Claerbout, 1985). Elboth delivered data denoising withinside the time-frequency domain (Elboth et al., 2008). Aghamiri offered a technique for removing the impact of residuals static through the usage of denoising in the f-x domain (Aghamiri and Gholami, 2016).

In 2018 a new technique with a niche genetic algorithm based on the Poisson disk sampling was presented. First, based on conventional residual static corrections, real number codes are calculated with the Poisson disk sampling to increase the uniformity of the preliminary solution. Then multi-populations of niches are constructed with multi-threads to estimate residual statics (Zhou et al., 2018). In 2019, diverse strategies were presented. Taking benefit of the matching pursuit algorithm in seismic signal decomposition

and reconstruction, CMP gathers are decomposed into unique atoms and the residual statics are implemented to every atom of CMP trace inside a certain time window (Zhao et al., 2019). Some other article, makes use of the statistics of high-SNR data first breaks to calculate residual statics of shot points or receivers. These techniques now no longer rely on surface models and have no limit of statics (Pan et al., 2019).

PRELIMINARIES

In this paper, small and capital letters x and A are used in bold, the former to indicate vectors and the latter for matrixes. The N-point signal x is signified as x = $[x_0,\ x_1, \dots, x_{N-1}]$. The elements of matrix A are illustrated as A_{ij} or $[\mathrm{A}_{ij}]$.

In this work, l_1 and l_2 are norms of x which are characterized as:

$$\|\mathrm{X}\|_1 = \sum_n |\mathrm{X}_n|\,, \qquad \|\mathrm{X}\|_2^2 = \sum_n |\mathrm{X}_n|^2 \quad . \tag{1}$$

As Figueiredo's work (Figueiredo et al., 2007) solves a sequence of minimization problems (MM method), we can minimize a challenging cost function F like this:

$$\mathrm{X}^{(r+1)} = argmin_x G\left(\mathrm{x}, \mathrm{x}^{(r)}\right) \quad , \tag{2}$$

$r \geq 0$ indicates the iteration counter.

DATUM ESTIMATION AND DENOISING: PROBLEM FORMULATION:

This work is based on modeling an N-point noise-free seismogram vector as:

$$\mathrm{s} = \mathrm{x} + \mathrm{f}\ , \quad \mathrm{s} \in \{\mathrm{R}\}^N \quad . \tag{3}$$

Vector f is a low-pass signal. vector x is designed as a sparse derivative signal which itself and its first multiple derivatives are sparse.

The noisy data is designed as:

$$\begin{aligned} \mathrm{d} &= \mathrm{s} + \mathrm{w} \\ &= \mathrm{x} + \mathrm{f} + \mathrm{w}, \qquad \mathrm{y} \in \{\mathrm{R}\}^{\mathrm{N}} \end{aligned} \tag{4}$$

and w is a stationary white Gaussian noise with variance σ^2. Now we have to evaluate f(datum) and x(peaks) at the same time from observation d.

Our assumption is: in absence of peaks, low-pass filtering can give the estimate of the datum from a noise-corrupted observation. So:

$$\hat{f} = L(d - \hat{x}). \tag{5}$$

We can find the estimate $\hat{\mathbf{s}}$ like this:

$$\begin{aligned} \hat{\mathbf{s}} &= \hat{\mathbf{f}} + \hat{\mathbf{x}} \\ &= \mathbf{L}(\mathbf{d} - \hat{\mathbf{x}}) + \hat{\mathbf{x}} \\ &= \mathbf{L}\mathbf{d} + \mathbf{H}\hat{\mathbf{x}} \end{aligned} \tag{6}$$

$\mathbf{H}$ is the high-pass filter:

$$\mathbf{H} = \mathbf{I} - \mathbf{L} \quad . \tag{7}$$

To estimate $\hat{\mathbf{x}}$ from observed data $\mathbf{d}$, we model an inverse problem with the quadratic data accuracy term $\|\mathbf{d} - \hat{\mathbf{s}}\|_2^2$. We have:

$$\begin{aligned} \|\mathbf{d} - \hat{\mathbf{s}}\|_2^2 &= \|\mathbf{d} - \mathbf{L}\mathbf{d} - \mathbf{H}\hat{\mathbf{x}}\|_2^2 \\ &= \|\mathbf{H}(\mathbf{d} - \hat{\mathbf{x}})\|_2^2 \end{aligned} \tag{8}$$

In this formulation, the data accuracy term depends on the high-pass filter H, also it does not depend on the datum estimate $\hat{\mathbf{f}}$. The optimization problem below provides an estimate of the peaks $\hat{\mathbf{x}}$. The datum estimate then will be obtained by (5).

Compound sparse derivative model

In (3), for the estimated peaks, $\hat{\mathbf{x}}$, the first $\boldsymbol{i}$ derivatives must be sparse. For the processing of sparse signals, we obtain the sparse signal behavior by using appropriate non-quadratic regularization terms. So, to achieve an estimated $\hat{\mathbf{x}}$, this optimization will be useful:

$$\hat{\mathbf{x}} = argmin_x \left\{ \boldsymbol{F}(\mathbf{x}) = \frac{\mathbf{1}}{\mathbf{2}} \|\mathbf{H}(\mathbf{d} - \mathbf{x})\|_2^2 + \sum_{\boldsymbol{i}=\mathbf{0}}^{\boldsymbol{N}} \boldsymbol{\tau_i} \mathbf{R}_{\boldsymbol{i}}(\mathbf{D_i x}) \right\} \tag{9}$$

$\boldsymbol{D_i}$ is the order –$\boldsymbol{i}$ difference operator.

$$\boldsymbol{R_i}(\mathbf{v}) = \sum_{\boldsymbol{n}} \Omega(\boldsymbol{v_n}) \tag{10}$$

Ω: $\mathbb{R} \rightarrow \mathbb{R}$ is a penalty function, substituting (10) in (9), we obtain:

$$\hat{\mathbf{x}} = argmin_x \left\{ \begin{array}{l} \boldsymbol{F}(\mathbf{x}) = \dfrac{\mathbf{1}}{\mathbf{2}} \|\mathbf{H}(\mathbf{d}-\mathbf{x})\|_2^2 \\ \\ +\displaystyle\sum_{\boldsymbol{i}=\mathbf{0}}^{\boldsymbol{N}} \boldsymbol{\lambda_i} \sum_{\boldsymbol{n}=\mathbf{0}}^{\boldsymbol{N_i}-\mathbf{1}} \Omega\left([\mathbf{D}_{\boldsymbol{i}}\mathbf{x}]\right)_{\boldsymbol{n}} \end{array} \right\} \tag{11}$$

where the constants $\boldsymbol{\lambda_i} \geq 0$ are regularization parameters and an increase in them makes the $\mathbf{D_i x}$ sparser. $\boldsymbol{N_i}$ indicates the length of $\mathbf{D_i x}$.

ALGORITHMS

Symmetric penalty functions

We have (Ning et al., 2014):

$$\begin{aligned} \sum_{\boldsymbol{n}} \boldsymbol{g}(\boldsymbol{x_n}, \boldsymbol{v_n}) &= \sum_{\boldsymbol{n}} \left[\frac{\Omega'(\boldsymbol{v_n})}{\mathbf{2}\boldsymbol{v_n}} \boldsymbol{x_n^2} + \Omega(\mathbf{v_n}) - \frac{\boldsymbol{v_n}}{\mathbf{2}} \Omega'(\mathbf{v_n}) \right] \\ &= \frac{\mathbf{1}}{\mathbf{2}} \mathbf{x}^{\mathbf{T}} [\boldsymbol{\Lambda}(\mathbf{V})] \mathbf{X} + \boldsymbol{c}(\mathbf{V}) \end{aligned} \tag{12}$$

Λ (v) is a diagonal matrix with diagonal elements and c(v) is the scalar.

$$[\boldsymbol{\Lambda}(\mathbf{V})]_{\mathbf{n,n}} = \frac{\Omega'(\mathbf{v})}{\mathbf{v_n}} \tag{13}$$

$$c(\mathrm{V}) = \sum_{n} [\Omega(v_n) - \frac{v_n}{2} \Omega'(\mathrm{v}_n)\ ] \tag{14}$$

Using (12) to (14), we have:

$$\begin{aligned} &\textstyle\sum_{i=0}^{N} \lambda_i \sum_{n=0}^{L_i-1} g([D_i x]_n, [D_i v]_n) = \sum_{i=0}^{N} \left[\frac{\lambda_i}{2} (D_i x)^T [\Lambda(D_i V)](D_i x) + c_i(V) \right] \\ &\qquad \geq \sum_{i=0}^{N} \lambda_i \sum_{n=0}^{L_i-1} \Omega([\mathrm{D}_i \mathrm{x}]_n) \end{aligned} \tag{15}$$

$\Lambda(D_i \mathrm{V})$ are diagonal matrices and $\boldsymbol{c_i}(\mathbf{V})$ are scalars,

$$[\Lambda(D_i x)]_{n,n} = \frac{\Omega'([D_i V]_n)}{[D_i V]_n} \tag{16}$$

$$c_i(\mathrm{V}) = \sum_n [\Omega([D_i \mathrm{V}]_n) - \frac{[D_i \mathrm{V}]_n}{2} \Omega'([D_i \mathrm{V}]_n)] \tag{17}$$

Equality holds when x = v. Eq. (15) shows:

$$\mathrm{G}\ (\mathrm{x},\ \mathrm{v})\ =\ 1/2\ \ \|\mathrm{H}(\mathrm{d}-\mathrm{x})\|_2^2 + \sum_{i=0}^{N}[\frac{\lambda_i}{2}(\mathrm{D}_i \mathrm{x})^T[\boldsymbol{\Lambda}(\mathrm{D}_i \mathrm{V})](\mathrm{D}_i \mathrm{x})] + C(\mathrm{V}) \tag{18}$$

Asymmetric and symmetric penalty functions

In the positivity of the seismogram peaks, it is better than applying the second form of BEADS. For this reason, we use an asymmetric penalty that penalizes negative values of x more than positive values.

$$\hat{\mathbf{x}} = argmin_x \left\{ \boldsymbol{F}(\mathbf{x}) = \frac{\mathbf{1}}{\mathbf{2}} \|\mathbf{H}(\mathbf{d}-\mathbf{x})\|_2^2 + \lambda_0 \sum_{n=0}^{L-1} \psi_\epsilon(\mathrm{x}_n;\ \mathrm{k}) + \sum_{i=1}^{N} \lambda_i \sum_{n=0}^{L_i-1} \Omega([D_i \mathrm{V}]_n) \right\} \tag{19}$$

we have:

$$\sum_{n=0}^{M-1} \mathrm{g}_0\ (\mathrm{x}_n, \mathrm{v}_n) = X^T[\Pi(\mathrm{V})]\mathrm{X} + \mathrm{b}^T\mathrm{x} + \mathrm{c}(\mathrm{v}) \geq \sum_{n=0}^{M-1} \psi_\epsilon(\mathrm{x}_n;\ \mathrm{k}) \tag{20}$$

$\Pi(\mathrm{V})$ is a diagonal matrix with diagonal elements, b is a vector with elements, and c(v) is a scalar that does not depend on x (Ning et al., 2014).

$$[\Pi(\mathrm{v})]_{n,n} = \begin{cases} \dfrac{1+k}{4|v_n|}, & |v_n| \geq \epsilon \\ \dfrac{1+k}{4\epsilon}, & |v_n| \leq \epsilon \end{cases} \tag{21}$$

and:

$$[\mathrm{b}]_n = \frac{1-k}{2} \tag{22}$$

PROOFS

Gaussian smoothing filter

A Gaussian filter is a filter whose impulse response is approximately a Gaussian function. It has the minimal possible group delay because it has the properties of having no overshoot to a step function input while minimizing the rise and fall time. Gaussian filter is taken into consideration as the appropriate time-domain filter, simply because the sinc is the appropriate frequency-domain filter. Mathematically, a Gaussian filter modifies the input signal through convolution with a Gaussian function. It is a low-pass linear filter used for noise reduction. As a Mexican hat, this filter has a climax and, on each side, it decreases quickly, Fig. 1. assuming data as one-dimensioned, the middle ones as of the highest weight, and as shifting to corners data weight reduce, this option preserves the edges and boundaries (Rakheja and Vig, 2016).

Two variables Gaussian filter indicates by:

$$G_0(\mathrm{x},\mathrm{y}) = \mathrm{A}e^{\frac{-(x-\mu_x)^2}{2\sigma_x^2}+\frac{-(y-\mu_y)^2}{2\sigma_y^2}} \tag{23}$$

In which μ is peak and σ is the variance and $A = 1/2\pi\sigma^2$.

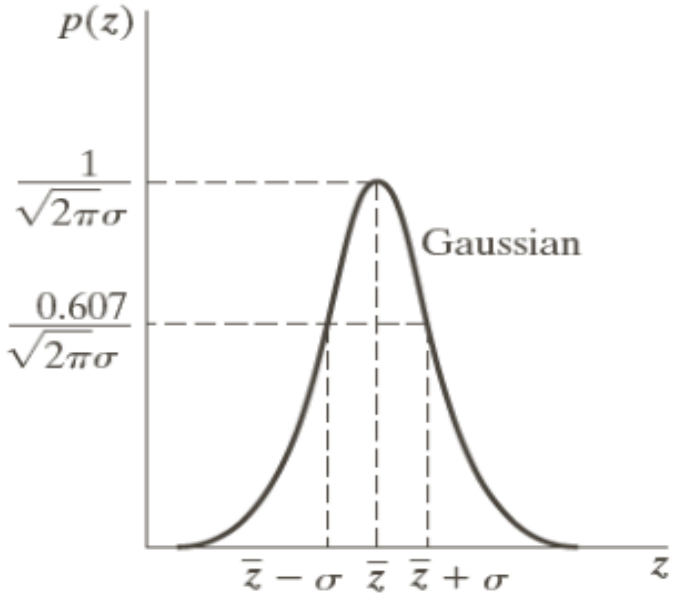

Fig. 1. Gaussian function (Rakheja and Vig, 2016).

Synthetic data

1. There are 2 methods to generate synthetic data, in both, it's far feasible to make the seismic data peaks. Making signal x with different amplitudes, widths, and positions as a superposition of Gaussian function. There are techniques to simulate the datum (Ning et al., 2014): Type 1 simulated datum: by the sum of an order-n polynomial, and an f-frequency sinusoidal signal, a data signal is made.

2. Type 2 simulated datum: a datum is made with a power spectrum limited to $[0,f_c]$ Which is a low-pass range, as a stationary random process. This kind of signal is achieved by applying a low-pass filter (with a cutoff frequency f_c) to a white Gaussian process.

3. If Gaussian white noise is added to each trace, we have noisy data. For each signal and SNR level, the BEADS is used to estimate the data, this gives us the estimated difference between the data and the peaks, which leads to the time change required for the static correction. The accuracy of this is assessed by identifying the SNR of the output. Fig. 2 shows the static residual correction of the seismic data simulated with BEADS. As may be seen, events are smoothed sufficient to be taken into consideration as static corrected, and noises are removed. The proposed method (BEADS), also can be in comparison with every other algorithm: The Gaussian method, it could be visible that on average, BEADS provides a slightly smaller error.

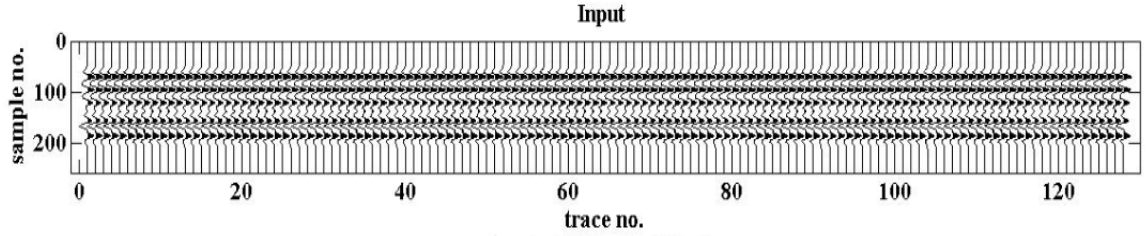

(a)

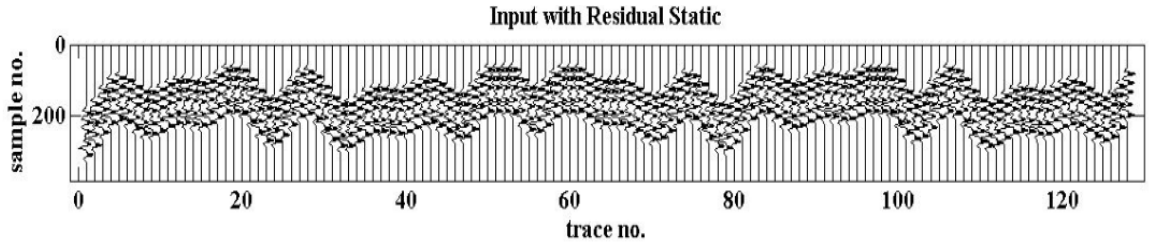

(b)

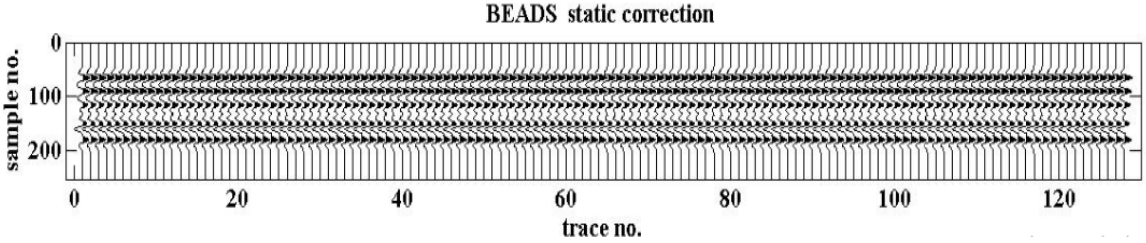

(c)

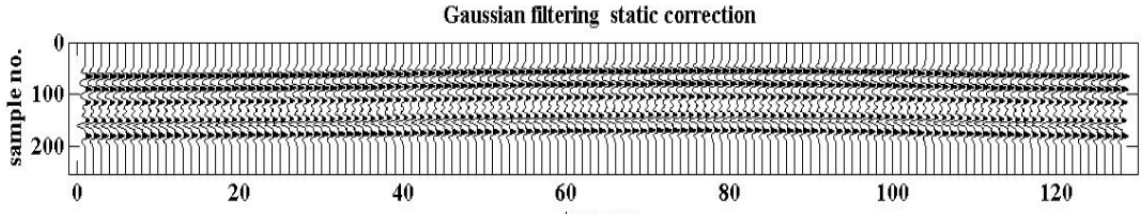

(d)

Fig. 2. BEADS static correction on synthetic data. (a) input, (b) before static correction, (c) after static correction using BEADS, (d) after static correction using Gaussian smoothing.

Real data

In Fig. 3 and Fig. 4 there is the impact of static correction using BEADS on single events of real records and in Fig. 5 total static of those events are illustrated:

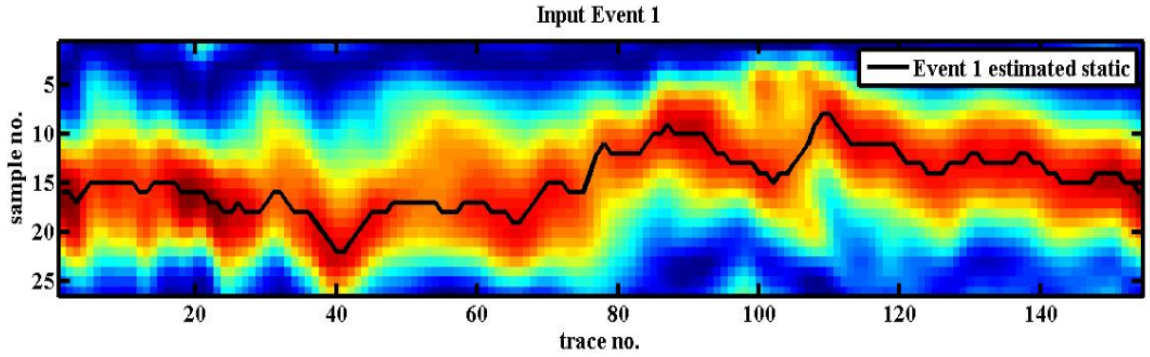

(a)

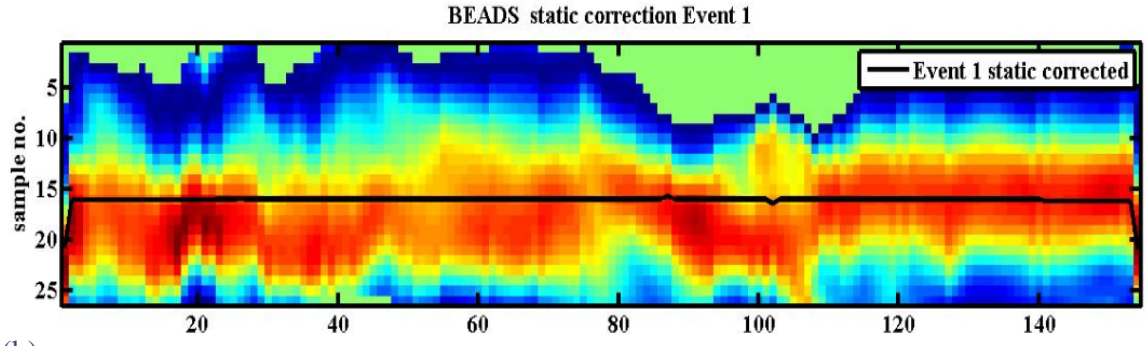

(b)

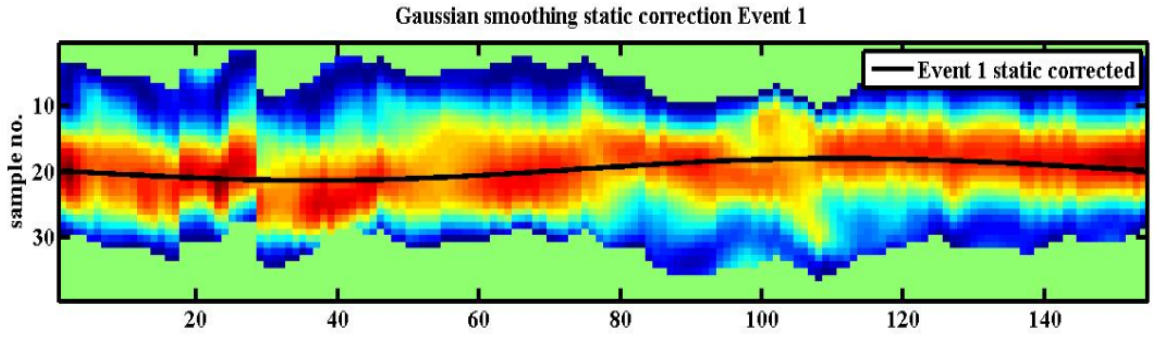

(c)

Fig. 3. (a) Real event before the static correction, (b) the same event after static correction using BEADS, (c) the same event after static correction using Gaussian smoothing.

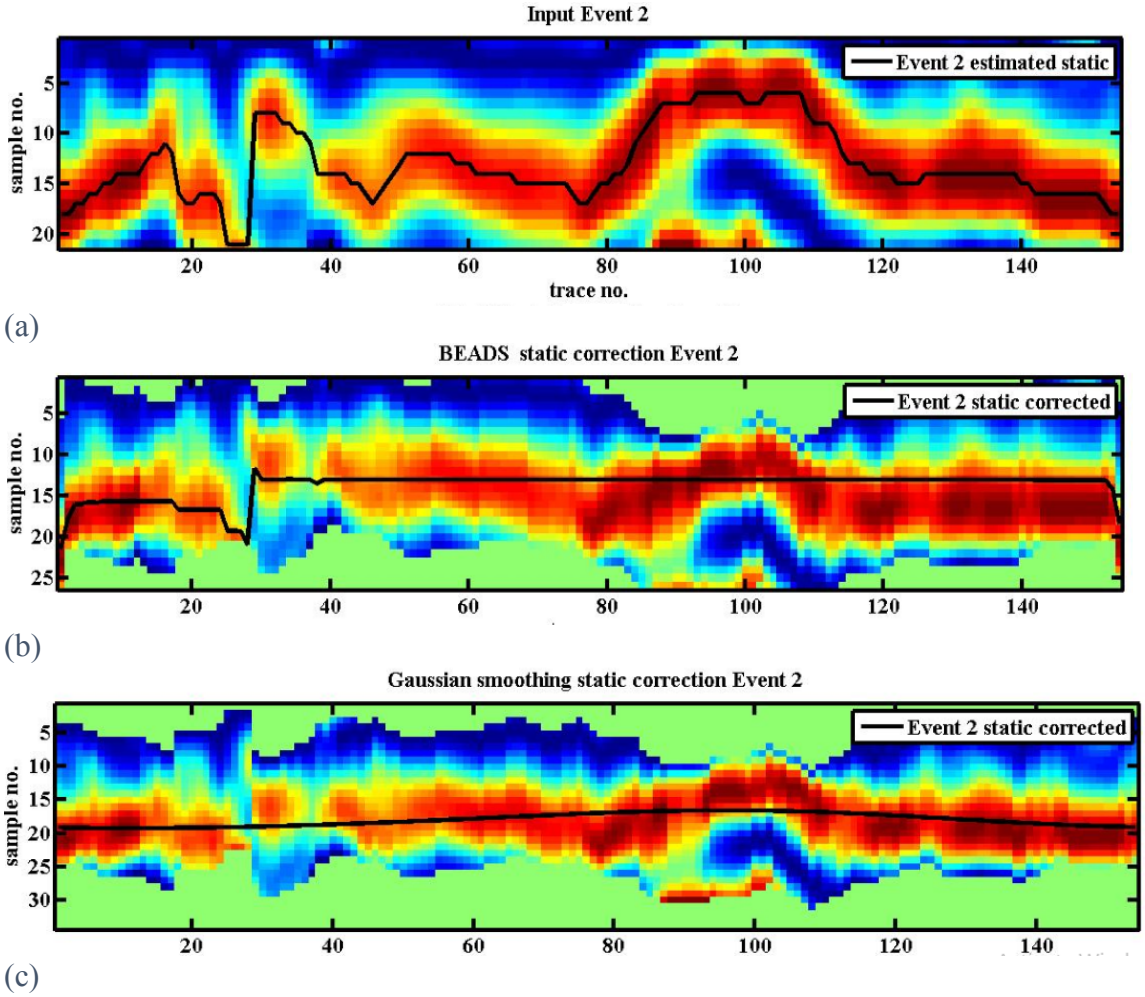

Fig. 4. (a) A real event before the static correction. (b) The same event after static correction using BEADS. (c) The same event after static correction using Gaussian smoothing.

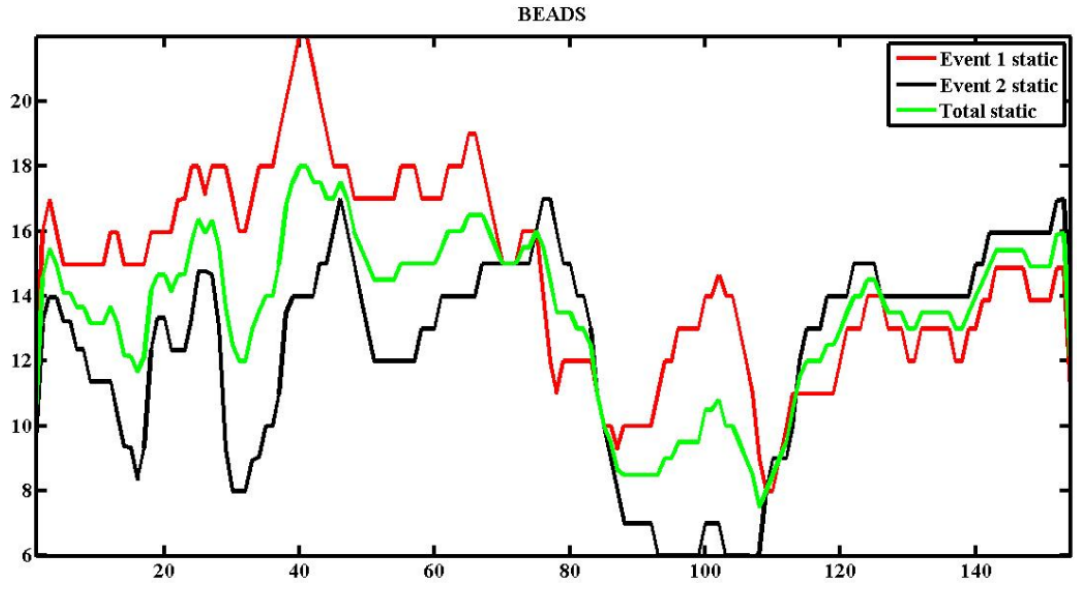

Fig. 5. Total static of the events in Fig. 3 and Fig. 4.

An efficient denoising technique reduces the wavelength of data to make it extra apparent in the trace, in Fig. 6 and Fig. 7 this trait of static correction using BEADS is shown:

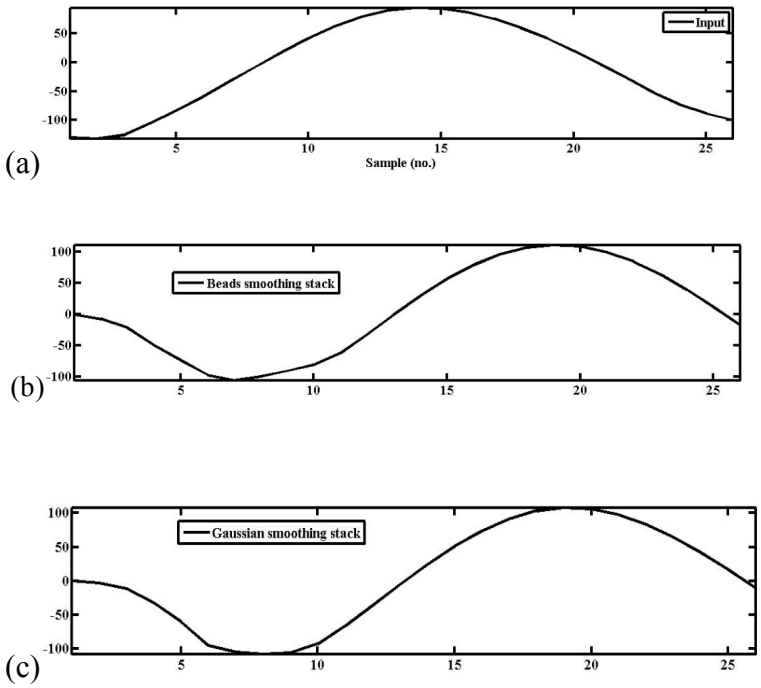

Fig. 6. (a) Wavelength of an event in input data, (b) its wavelength after applying BEADS, (c) after applying Gaussian smoothing.

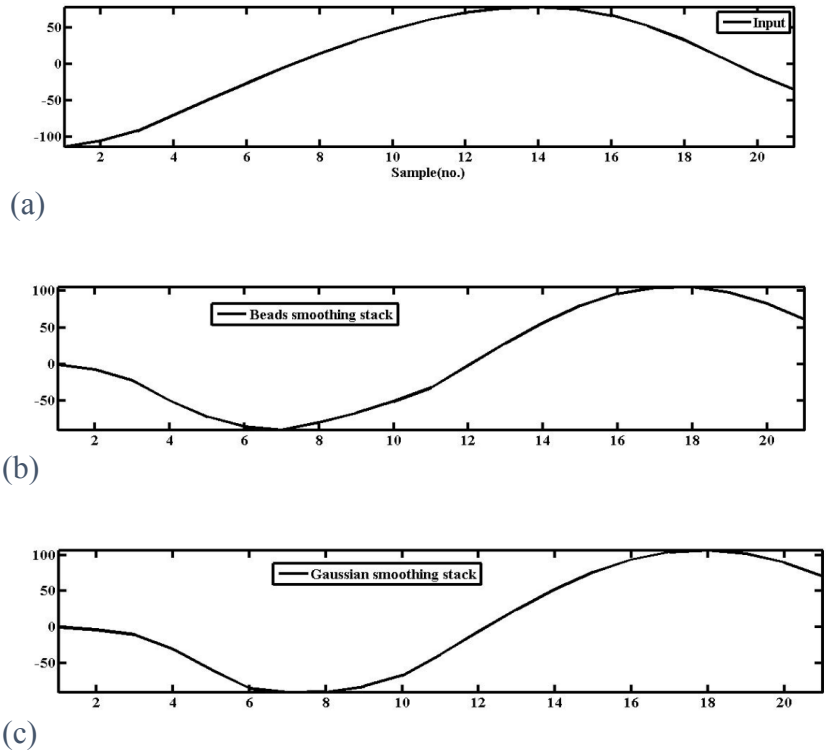

Fig. 7. (a) Wavelength of an event in input data, (b) its wavelength after applying BEADS, (c) after applying Gaussian smoothing.

After stacking, the larger amplitude yields the greater apparent events in the seismic trace, and BEADS could make an increase in event amplitudes. In Fig. 8, input stacked data is shown in blue and the static corrected stacked data after as the use of the proposed method is illustrated through black, the variations among amplitudes may be seen. Statics take into consideration as high-frequency noises, so we should eliminate the high-frequency part of input data to acquire smooth events, as in Fig. 9 the amplitude in the high frequencies is mitigated (power in the vertical axis is amplitude to the power of two).

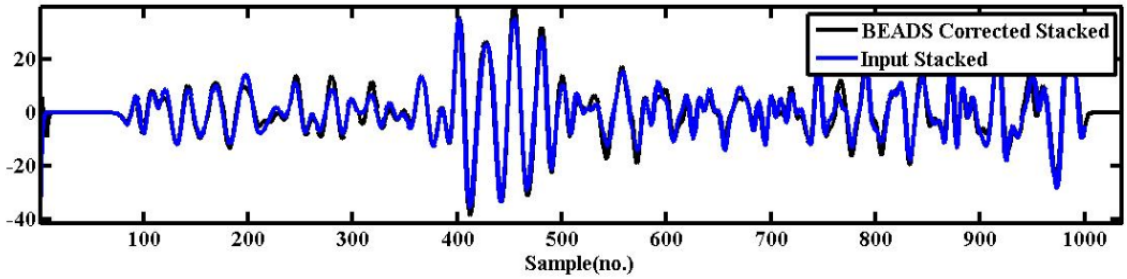

Fig. 8. Blue one - stacked data. Black one - the same data after BEADS static correction and stack.

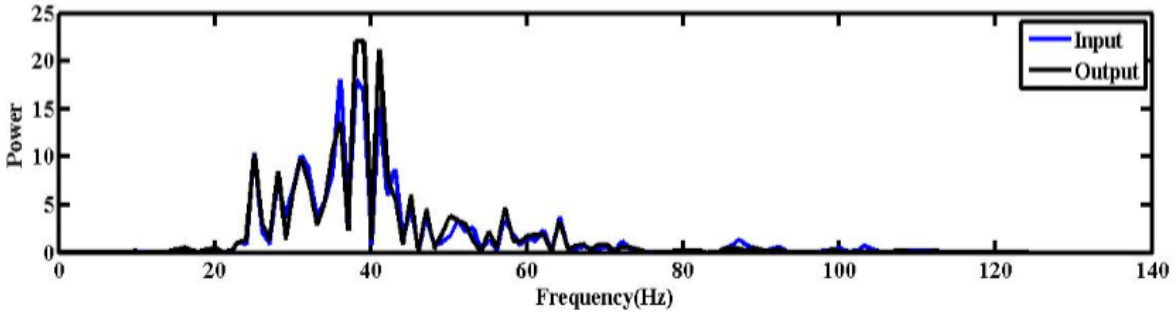

(a)

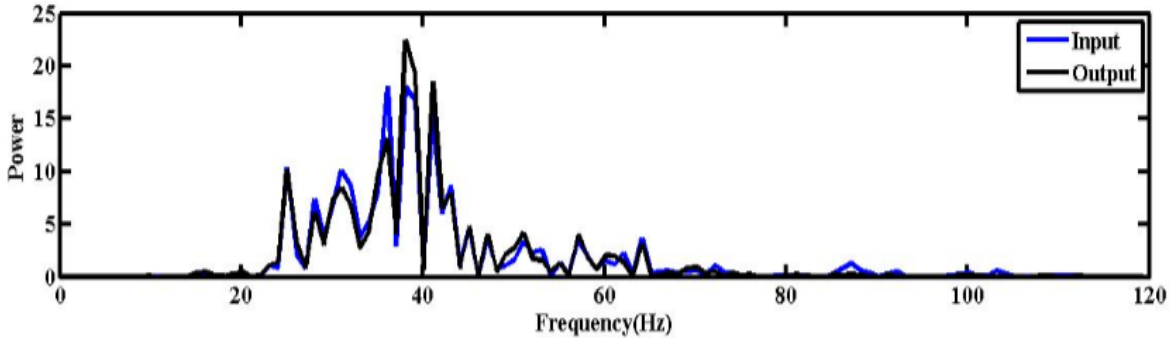

(b)

Fig. 9. (a) Power in terms of frequency. The blue one - before the static correction, the black one-after static correction using BEADS. (b) The blue one - before the static correction, the black one - after static correction using Gaussian smoothing.

In Fig. 10 we have shown real seismic data (a) and the same trace after applying residual static correction using the BEADS method. There are some obvious differences between them, which show that more events are visible and aligned.

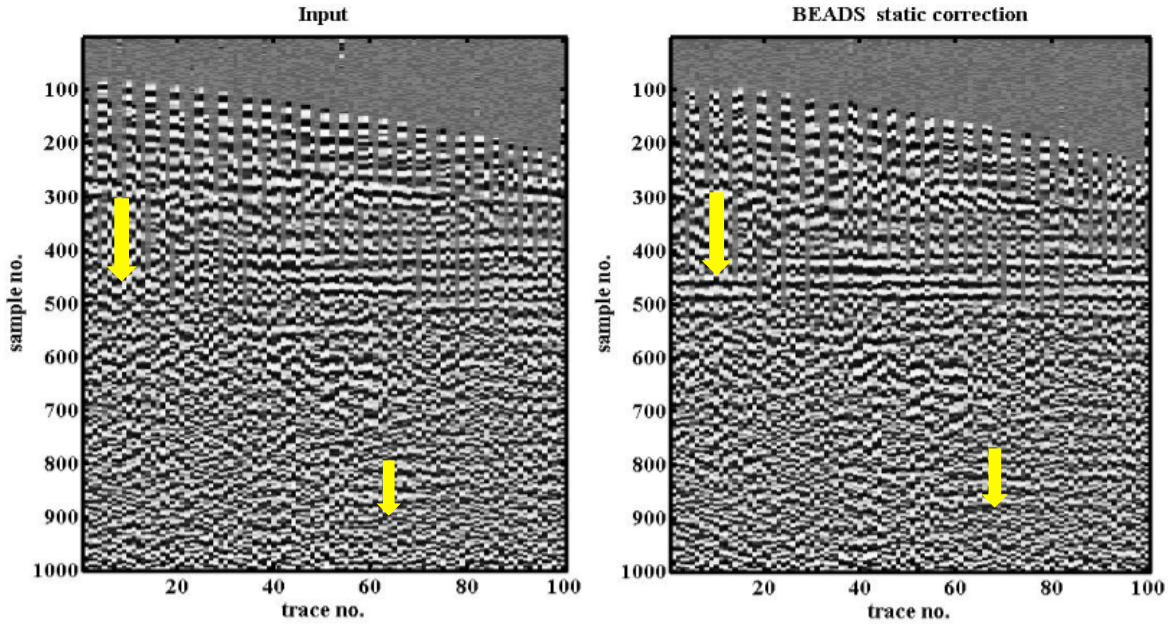

Fig. 10. (a) Real seismic data and (b) after static correction using BEADS.

CONCLUSION

In this paper, we have addressed the residual static correction problem in the case of noise reduction. The proposed technique is primarily based totally on non-parametric models for the seismogram peaks and mainly datum that is modeled as a low-pass signal and the series of seismogram peaks is modeled as sparse and having sparse derivatives. In addition, to make sure of the positivity of seismogram peaks, we used both asymmetric and symmetric penalty functions. The problem is formulated as banded matrices so that the iterative optimization is computationally efficient, can be applied for long data series, and uses much less memory. The overall performance of the datum correction is assessed on simulated seismic records and in comparison, with different methods. It may be visible from experiments that the recommended technique can estimate the datum of real seismogram a lot higher and because it estimates the datum and the seismograms peaks jointly, it could carry out noise reduction and datum correction simultaneously. This technique additionally may be modeled for different kinds of signals by customizing penalty functions and regularization parameters (λ_i). It makes use of asymmetric and symmetric penalty functions to assure the positivity of the expected peak. By estimating the datum and peaks we will achieve the time shifts necessary for static correction.

REFERENCES

Aghamiri, S.H. and Gholami, A., 2016. Residual static correction using denoising in the f-x domain. J. Res. Appl. Geophys., 2: 1-9. DOI: 10.22044/JRAG.2016.652

Barwick, V.J., 1999. Sources of uncertainty in gas chromatography and high-performance liquid chromatography. J. Chromatogr. A, 849: 13-33.

Bioucas-Dias, J.M. and Figueiredo, M.A.T., 2008. An iterative algorithm for linear inverse problems with compound regularizers. Proc. Internat. Conf. Image Process.: 685-688.

Brown, C.D., Vega-Montoto, L. and Wentzell, P.D., 2000. Derivative preprocessing and optimal corrections for baseline drift in multivariate calibration. Appl. Spectrosc., 54: 1055-1068.

Cappadona, S., Levander, F., Jansson, M., James, P., Cerutti, S. and Pattini, L., 2008. Wavelet-based method for noise characterization and rejection in high-performance liquid chromatography coupled to mass spectrometry. Anal. Chem., 80: 4960-4968.

Chan, T.F., Osher, S. and Shen, J., 2001. The digital TV filter, and nonlinear denoising. IEEE Trans. Image Process, 10: 231-241.

Chau, F.T. and Leung, A.K.-M., 2000. Application of wavelet transform in processing chromatographic data. In: Walczak, B. (Ed.), Wavelets in Chemistry. Elsevier Science Publishers, Amsterdam: 205-223. DOI:10.1016/S0922-3487(00)80034-9.

Chen, S.S., Donoho, D.L. and Donoho, M.A., 1998. Atomic decomposition by basis pursuit. SIAM J. Sci. Comput., 20: 33-61.

Elboth, T., Qaisrani, H.H. and Hertweck, T., 2008. De-noising seismic data in the time-frequency domain. Expanded Abstr., 78th Ann. Internat. SEG Mtg., Las Vegas. Doi: doi.org/10.1190/1.3063887.

Felinger, A., 1998. Data Analysis and Signal Processing in Chromatography. Elsevier Science Publishers, Amsterdam.

Figueiredo, M.A.T., Bioucas-Dias, J.M. and Nowak, R.D., 2007. Majorization–minimization algorithms for wavelet-based image restoration. IEEE Transact. Image Process., 16: 2980-2991.

Fischer, R., Hanson, K., Dose, V. and von der Linden, W., 2000. Background estimation in experimental spectra. Phys. Review E, 61: 1152-1160.

Gan, F., Ruan, G. and Mo, J., 2006. Baseline correction by improved iterative polynomial fitting with automatic threshold. Chem. Intell. Lab. Syst., 82: 59-65.

Gulam Razul, S., Fitzgerald, W.J. and Andrieu, C., 2003. Bayesian model selection and parameter estimation of nuclear emission spectra using RJMCMC. Nucl. Instrum. Meth. Phys., 497: 492–510.

Hatherly, P.J., Urosevic, M., Lambourne, A. and Evans, B.J., 1994. A simple approach to calculating refraction statics corrections. Geophysics, 59: 156-160.

Hu, Y., Jiang, T., Shen, A., Li, W., Wang, X. and Hu, J., 2007. A background elimination method based on wavelet transform for Raman spectra. Chemometr. Intell. Lab. Syst., 85: 94-101.

Kneen, M.A. and Annegarn, H.J., 1996. Algorithm for fitting XRF, SEM and PIXE X-ray spectra backgrounds. Nucl. Instr. Meth. Phys. Res. Sect. B.: 209–213.

Kutyniok, G., 2014. Geometric separation by single-pass alternating thresholding. Appl. Computat. Harmon. Analys., 36: 23-50.

Laeven, J.M. and Smit, H.C., 1985. Optimal peak area determination in the presence of noise. Anal. Chim. Acta, 176: 77-104. doi.org/10.1016/S0003-2670(00)81636-0.

Liu, Y., Cai, W. and Shao, X., 2013. Intelligent background correction using an adaptive lifting wavelet. Chemometr. Intell. Lab. Syst., 25: 11-17.

Mazet, V., Carteret, C., Brie, D., Idier, J. and Humbert, B., 2005. Background removal from spectra by designing and minimizing a non-quadratic cost function. Chemometr. Intell. Lab. Syst., 76. 121–133

McNulty, D.A. and MacFie, H.J.H., 1998. The effect of different baseline estimators on the limit of quantification in chromatography. J. Chemomet., 11: 1-11.

Moore, A.W. and Jorgenson, J.W., 1993. Median filtering for removal of low-frequency background drift. Analyt. Chem., 65: 188-191.

Ning, X., Selesnick, I. and Duval, L., 2014. Chromatogram baseline estimation and denoising using sparsity (BEADS). Chemometr. Intell. Lab. Syst., 139: 156-167.

Pan, L., Liu, Y., Zheng, H., Zhao, Y. and Guo, Q., 2019. First-break residual static corrections applied in the southern part of Anjihai area. Geophys. Prosp., 54: 274-279.

Rakheja, P. and Vig, R., 2016. Image denoising using combination of median filtering and wavelet transform. Int. J. Comput. Appl., 141(9).

Ronen, J. and Claerbout, J.F., 1985. Surface-consistent residual statics estimation by stack-power maximization. Geophysics, 50: 2759-2767.

de Rooi, J.J. and Eilers, P.H.C., 2012. Mixture models for baseline estimation. Chemometr. Intell. Lab. Syst., 117: 56-60.

Ruckstuhl, A.F., Jacobson, M.P., Field, R.W. and Dodd, J.A., 2001. Baseline subtraction using robust local regression estimation. J. Quantit. Spectrosc. Radiat. Transf., 68: 179-193.

Smite, H.C. and Steigstra, H., 1988. Noise and detection limits in signal-integrating analytical methods. In: Currie, L.A. (Ed.), Detection in Analytical Chemistry: Importance, Theory, and Practice. ACS Symposium Series, American Chemical Soc.: 126-148. DOI: 10.1021/bk-1988-0361.ch007.

Wiggins, R.A., Larner, K.L. and Wisecup, R.D., 1976. Residual statics analysis as a general linear inverse problem. Geophysics, 41: 922-938.

Zhang, Z.M., Chen, S. and Liang, Y.Z., 2010. Baseline correction using adaptive iteratively reweighted penalized least squares. The Analyst, 135: 1138-1146. DOI: 10.1039/b922045c.

Zhao, J., Li, J. and Cheng, J., 2019. Seismic gathers residual static correction based on matching pursuit algorithm. Expanded Abstr., 89th Ann. Internat. SEG Mtg., San Antonio: 2918-2922.

Zhou, Q., Cao, L. and Chen, A., 2018. Residual static corrections with the niche genetic algorithm based on Poisson disk sampling. Geophys. Prosp., 53: 896-902. DOI: 10.13810/j.cnki.ISSN.1000-7210.2018.05.002